Volume 7 | Number 11 | November 2019 | Pages 4401–4828

# Biomaterials Science

rsc.li/biomaterials-science

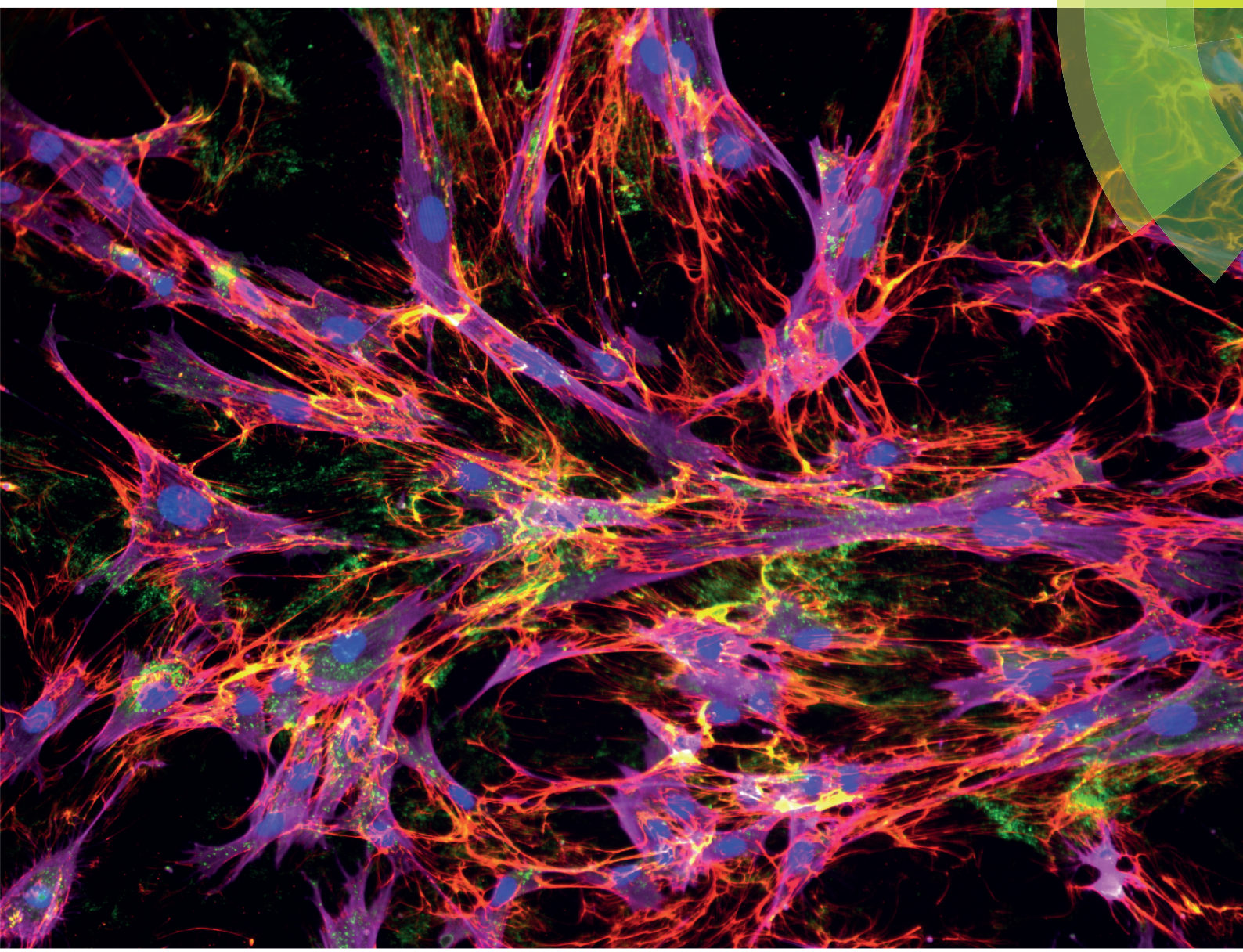

ISSN 2047-4849

ROYAL SOCIETY OF CHEMISTRY | Celebrating IYPT 2019

PAPER
Viola Vogel *et al.*
Fibrillar fibronectin plays a key role as nucleator of collagen I polymerization during macromolecular crowding-enhanced matrix assembly

ESB European Society for Biomaterials

Biomaterials Science

PAPER

View Article Online
View Journal | View Issue



Cite this: *Biomater. Sci.*, 2019, **7**, 4519

# Fibrillar fibronectin plays a key role as nucleator of collagen I polymerization during macromolecular crowding-enhanced matrix assembly†

Jenna Graham, [a] Michael Raghunath [b] and Viola Vogel *[a]

Macromolecular crowding is used by tissue engineers to accelerate extracellular matrix assembly *in vitro*, however, most mechanistic studies focus on the impact of crowding on collagen fiber assembly and largely ignore the highly abundant provisional matrix protein fibronectin. We show that the accelerated collagen I assembly as induced by the neutral crowding molecule Ficoll is regulated by cell access to fibronectin. Ficoll treatment leads to significant increases in the amount of surface adherent fibronectin, which can readily be harvested by cells to speed up fibrillogenesis. FRET studies reveal that Ficoll crowding also upregulates the total amount of fibronectin fibers in a low-tension state through upregulating fibronectin assembly. Since un-stretched fibronectin fibers have more collagen binding sites to nucleate the onset of collagen fibrillogenesis, our data suggest that the Ficoll-induced upregulation of low-tension fibronectin fibers contributes to enhanced collagen assembly in crowded conditions. In contrast, chemical cross-linking of fibronectin to the glass substrate prior to cell seeding prevents early force mediated fibronectin harvesting from the substrate and suppresses upregulation of collagen I assembly in the presence of Ficoll, even though the crowded environment is known to drive enzymatic cleavage of procollagen and collagen fiber formation. To show that our findings can be exploited for tissue engineering applications, we demonstrate that the addition of supplemental fibronectin in the form of an adsorbed coating markedly improves the speed of tissue formation under crowding conditions.

Received 4th June 2019,
Accepted 2nd August 2019

DOI: 10.1039/c9bm00868c

rsc.li/biomaterials-science



## Introduction

Since the *in vitro* growth of engineered tissue substitutes is time consuming and thus expensive, a primary challenge taken on by tissue engineers is to define methods to speed up the assembly of native extracellular matrix (ECM) by cells *in vitro*. Important factors contributing to the success of a tissue engineered product besides the speed of assembly are its physical stability, how close the physical and biochemical properties are to native ECM, cell viability, cell proliferation, and cell phenotype. In recent years, macromolecular crowding has been applied to tissue engineering to improve the success of tissue assembly *in vitro*.[1–3] Molecular crowding results in much faster ECM assembly, as well as more native matrix architecture, enhanced matrix remodeling, and reduced cellular phenotypic drift (see ESI Table 1† for a summary of literature concerning the use of crowding in tissue engineering).

The term macromolecular crowding describes the phenomenon where soluble macromolecules in a fluid take up space (excluded volume) and thereby affect the behavior of neighboring molecules whose available volume and thus conformational freedom are decreased,[4,5] resulting in more compact protein conformations. Crowding also slows diffusion, enhances the interaction of molecules, their aggregation, and enhances adsorption of proteins onto surfaces.[4,6–10] Since the *in vivo* extracellular environment contains 9%–45% volume fraction of macromolecules (FVO),[11] various artificial crowding agents have been added to cell culture to mimic *in vivo* crowding. One of the most commonly used crowding mimics is a mixture of two types of Ficoll (ESI Table 1†), a neutral, synthetic polysucrose[12–17] that has been FDA approved for clinical and *in vitro* applications.[18,19] The mixture of 37.5 mg mL$^{-1}$ 70 kDa and 25 mg mL$^{-1}$ 400 kDa Ficoll creates a crowded solution with an FVO of approx. 18% v/v which replicates the crowding level in blood plasma[2,12,20] and has proven effective in enhancing matrix assembly.[11–17,21–23] Even though negatively charged crowding molecules like carrageenan have a stronger enhancing effect on matrix assembly, they have an unequal

[a]*Department of Health Sciences and Technology, ETH Zürich, CH-8093 Zürich, Switzerland. E-mail: viola.vogel@hest.ethz.ch*
[b]*ZHAW School of Life Sciences and Facility Management, Institute for Chemistry and Biotechnology, Center for Cell Biology and Tissue Engineering, CH-8820 Wädenswil, Switzerland*

†Electronic supplementary information (ESI) available. See DOI: 10.1039/C9BM00868C

impact on different matrix components (*e.g.* they have a much stronger enhancing effect on collagen I than fibronectin) and therefore result in a change in the composition of the ECM.[22,24–26]

Crowding has been shown to enhance the assembly of a wide range of ECM molecules, including fibronectin, collagen types I–VII, laminin, fibrillin, vitronectin, heparin sulfate proteoglycan, hyaluronic acid, decorin, lysyl oxidase, tenascin C, and thrombospondin (see Chen *et al.*[2] for a more complete list). However, it is best described how crowding enhances assembly of collagen type I. Crowding enhances enzymatic cleavage of cell-secreted procollagen, both in a cell-free collagen gel assay and in cell culture,[1,2,20,21,27–29] and crowding promotes collagen self-association in cell-free systems.[2,30,31] Additionally, crowding increases transglutaminase 2 and lysyl oxidase cross-linking of collagen, as shown in cell culture.[1,2] Finally, a fragment produced from the activation of procollagen C proteinase enhancer 1 has been found to act as a matrix metallopeptidase 2 inhibitor,[21,32] thereby reducing the enzymatic digestion of the assembled collagen matrix.

In contrast to collagen, how crowding increases the assembly of fibronectin is not known. Fibronectin is the very first matrix molecule actively assembled into provisional ECM fibers by cells.[33–37] Though crowding drives supramolecular assembly, and should thus increase fibronectin–fibronectin binding, fibronectin fibrillogenesis is tightly regulated and requires fibronectin stretching to expose cryptic Fn–Fn binding sites.[38–42] Additionally, there is no enzymatic cleavage required to initiate fibronectin assembly, so crowding cannot be acting on fibronectin through this known mechanism. Given the important role of cell–fibronectin interactions in fiber assembly, crowding likely has another mechanism to increase fibronectin assembly that has not yet been identified.

It is also unknown what role fibronectin might play in the assembly of other ECM molecules in the presence of crowding. In early phases of ECM assembly, the initiation of collagen I polymerization into fibers needs to be nucleated. The nucleation of collagen I polymerization *in vivo* is initiated by fibronectin fibers which act as templates for collagen peptides to bind, similarly to the role of seeds that initiate biomineralization processes. In fact, even though collagen gels can be formed from a solution of collagen monomers *in vitro*, *i.e.* by lowering the pH and increasing the temperature, these initiation conditions are not typically exploited in cell culture and collagen matrix cannot be formed *in vivo* without the presence of fibronectin.[43–46] Importantly, though, early fibronectin-collagen binding is mechano-regulated as collagen peptides can tightly bind only to structurally relaxed but not to highly stretched fibronectin fibers.[35,47] Additionally, fibronectin binds to and enhances the procollagen cleavage activity of bone morphogenic protein 1 [48,49] and plays a role in regulating the activity of the collagen cross-linker lysyl oxidase.[50]

Given the significant interactions between fibronectin and collagen during matrix assembly, we asked here for the first time how fibronectin might regulate crowding-enhanced collagen I matrix assembly. To gain insights to how crowding increases fibronectin assembly over time, we supplemented fluorescently labeled fibronectin isolated from human plasma[51] to the cell media. We explored how crowding affects crucial mechanical cell functions and the cell ability to scrape off fibronectin from the substrate. Since fibronectin tension regulates the nucleation of collagen I polymerization, we next used our well-validated fibronectin-FRET probe[40,47,51–62] to assess how crowding affects the tensional state of fibronectin fibers within the matrix. We then manipulated the matrix assembly process in the presence of crowding by adjusting the adhesion of fibronectin to the glass substrate surface to assess the role of fibronectin fibers *versus* surface adsorbed fibronectin coating in matrix assembly. Finally, we explored how our findings might be exploited for tissue engineering applications.

## Results

### Ficoll increases assembly of fibronectin and collagen I fibers in the first 16 hours and they are colocalized

To take a close look at the impact of crowding on the early phases of ECM assembly, and particularly the interaction between fibronectin and collagen I, we cultured primary human dermal fibroblasts in the absence or presence of the standard Ficoll mixture (37.5 mg $mL^{-1}$ 70 kDa + 25 mg $mL^{-1}$ 400 kDa, GE Healthcare). Before adding fibroblasts, we adsorbed human plasma fibronectin to the glass substrate (50 μg $mL^{-1}$, 1 hour). It was previously shown that fibroblasts harvest fibronectin from the substrate surface and incorporate it into fibers, along with soluble plasma fibronectin from serum and their own cell produced cellular fibronectin,[63,64] as also observed here (ESI Movie 1†). Note in ESI Movie 1† that the cells stop scraping off fibronectin from the surface while rounding up and going through a cell division. We then sparsely seeded fibroblasts at 5000 cells per $cm^2$ and allowed them to adhere for 1 hour. We chose to start with a very low cell seeding density to allow for better visualization of the interaction of fibroblasts with the fibronectin coating and early matrix assembly. Next, the media were exchanged and fibroblasts were exposed to Ficoll (+Ficoll) or cultured in standard medium without crowders (−Ficoll). In both cases, 50 μg $mL^{-1}$ of human plasma fibronectin and 100 μM L-ascorbic acid 2-phosphate were supplemented to the cell culture media to promote matrix assembly. A small portion (10%) of the fibronectin supplemented to the media and in the coating was fluorescently labeled (Alexa-647) to enable its visualization. Significant matrix assembly took place during the first 16 hours, both in the absence and presence of Ficoll (Fig. 1A and B). Early fibronectin and collagen I fibers were colocalized in both conditions, as shown by the intensity linescans in Fig. 1A and B and by ESI Movie 2.† Ficoll did not have an impact on cell density after 16 hours (Fig. 1C). Quantification of fibronectin and collagen I by summing the respective fluorescent pixel intensities showed that there was already more of both matrix proteins with Ficoll treatment after only 16 hours

 

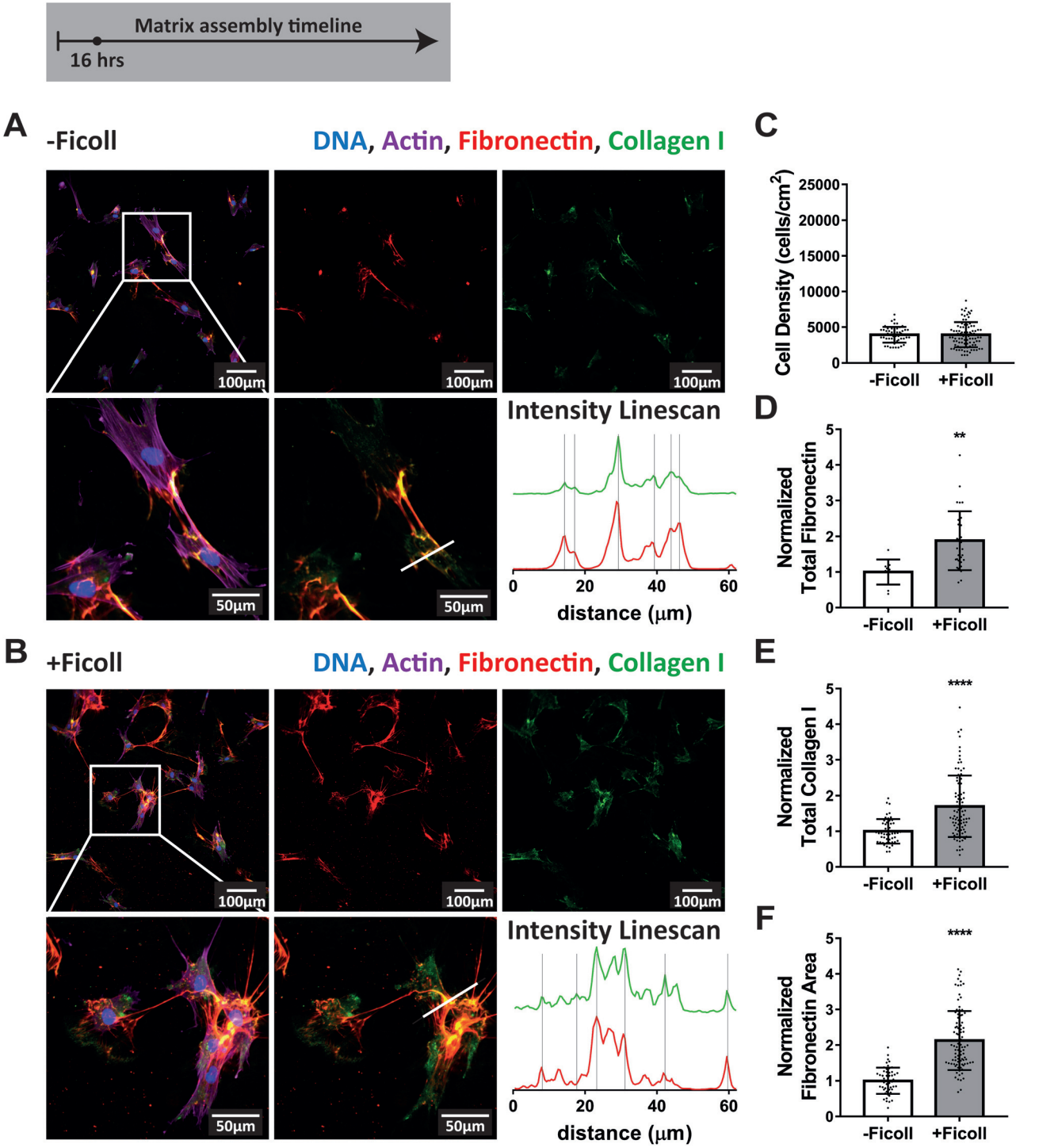


**Fig. 1** Ficoll supplementation accelerates ECM assembly within the first 16 hours and fibronectin and collagen I are colocalized. (A) ECM assembled without Ficoll. The first row shows a widefield fluorescence image of fibroblasts and matrix followed by images of Alexa-647-labeled fibronectin and antibody-stained collagen I alone. The second row shows a magnified area of the image above, followed by an image of matrix only and intensity linescans of fibronectin and collagen I along the white line indicated in the matrix only image to the left. (B) ECM assembled with Ficoll mixture (37.5 mg $mL^{-1}$ 70 kDa Ficoll + 25 mg $mL^{-1}$ 400 kDa). (C) Cell density. (D) Summed intensity of Alexa-647-labeled fibronectin. (E) Summed intensity of antibody-stained collagen I. (F) Area of substrate covered by fibronectin fibers as quantified using a threshold set to distinguish fibers from background and coating. 30–100 images were analyzed for each condition (10 for total fibronectin in -Ficoll condition). D–F show values normalized to the mean without Ficoll. Glass substrates preadsorbed with 50 μg $mL^{-1}$ plasma fibronectin (10% Alexa-647-labeled). Cells cultured in MEM Alpha supplemented with 10% fetal bovine serum, 1% penicillin–streptomycin, 100μM L-ascorbic acid 2-phosphate, and 50 μg $mL^{-1}$ plasma fibronectin (10% Alexa-647-labeled). **indicates $p < 0.01$, ****indicates $p < 0.0001$. Respective greyscale images of each channel can be found in ESI Fig. 1.† ESI Movie 2† shows alternating images of fibronectin and collagen I to appreciate their spatial correlation. Fibronectin matrix quantification by antibody staining can be found in ESI Fig. 4.†

(Fig. 1D and E). Notably, the effect of Ficoll on fibronectin deposition was stronger than on collagen I (1.9× *vs.* 1.7×, respectively). Additionally, the fibronectin matrix assembled with Ficoll covered approximately twice the area of that assembled without Ficoll (2.1×, Fig. 1F).

### Collagen I fibers mostly continue to colocalize with fibronectin fibers after 2 days of Ficoll exposure

Assembly of fibronectin and collagen I fibers remained enhanced under Ficoll treatment as fibroblasts were cultured for 2 days with respect to the control (Fig. 2). Importantly, as matrix assembly progressed, collagen I was still colocalized with fibronectin during the first few days, as shown by the intensity line scans in Fig. 2A and B and by ESI Movie 3.† Cell density had more than doubled since 16 hours and was still not impacted by Ficoll (Fig. 2C). Quantification of matrix proteins showed that Ficoll increased fibronectin fiber assembly more than collagen I also at this time point (2.6× *vs.* 1.8×, Fig. 2D and E). Ficoll induced fibronectin matrix covered about twice the area compared to the control without Ficoll (Fig. 2F).

### A dense ECM was assembled in 6 days both with and without Ficoll

To ask how effective Ficoll treatment is during the early *versus* late phases of cell culture, we continued the experiment further to six days, at which point the fibroblasts had reached confluence and developed a very dense matrix (Fig. 3A and B). The collagen I fibers showing the brightest immunolabel signal were still generally in close proximity to the fibronectin fibers, both with and without Ficoll, as can be appreciated in the *z*-stack shown in ESI Movie 4.† However, the depth and density of the ECM made it difficult to determine if collagen I was still strictly co-localized with fibronectin. Previous studies suggest that, by this time point, collagen I fibers have become increasingly interconnected and are no longer restricted to the fibronectin template.[47] After 6 days, fibroblasts had reached a confluent state and the cell density was the same with and without Ficoll (Fig. 3C). Quantification of fibronectin and collagen I showed that matrix assembly in non-Ficoll treated samples caught up significantly and the differences with Ficoll were quite small compared to earlier time points (Fig. 3D and E). Taken together, this time series from 16 hours to 6 days (Fig. 1–3) highlights the fact that Ficoll substantially accelerated the early matrix assembly process, while its effect evened out by 6 days when non-Ficoll-treated cultures caught up in terms of matrix assembly. ESI Fig. 4† shows that the results were the same when fibronectin was quantified not by Alexa-647-labeling of plasma fibronectin, but by antibody staining, as is standard in the field.

### Increased fibronectin fiber assembly is not attributable to changes in selected fibroblast functions

Given that fibronectin fibrillogenesis depends on traction forces, we next asked whether Ficoll upregulates cell contractility or any other cell functions related to matrix assembly. We cultured cells as before, except without fibronectin supplementation since this is not standard in the field, and analyzed them after 24 hours exposure to Ficoll. We measured cell spreading area and found no change with Ficoll (Fig. 4A). We then measured phosphorylation of focal adhesion kinase (pFAK), which is downstream of integrin ligation,[65] and found that this was also not changed by Ficoll treatment (Fig. 4B). We then assessed cell contractility by measuring the phosphorylation of myosin light chain 2 (p-MLC2), which was unchanged (Fig. 4C), as well as the amount of filamentous actin (F-actin) per cell, which increases with cell traction forces, and also remained unchanged (Fig. 4D). Fibroblasts could also have increased migration and/or membrane activity that results in increased harvesting of the fibronectin coating. We estimated the area of coating harvested per cell by dividing the total area per image where the fibronectin coating had been removed by the number of cells in that image. This was also unchanged with Ficoll (Fig. 4E). We then measured several nuclear markers that are known to be sensitive to mechanical interactions of cells with their environment. We found no significant changes in the ratio of lamin A to lamin B, the nuclear-to-cytoplasmic ratio of transcription factors yes-associated protein (YAP) and myocardin-related transcription factor-A (MRTF-A), or the histone markers acetylation of histone 3 at lysine 9 (H3K9Ac) and trimethylation of histone 3 at lysine 27 (H3K27me3) (Fig. 4F–J). Taken together, these results show that there were no apparent changes in cell behavior that could explain the increased fibronectin fiber assembly with Ficoll.

### Ficoll increases the amount of fibronectin at the glass surface where it is easily accessible for cell mediated fiber assembly

Next we asked whether Ficoll regulates cell access to fibronectin since crowding has been shown to increase the adsorption of molecules from the bulk fluid onto surfaces.[66,67] In order to assemble fibers, cell surface integrins need to bind to fibronectin, much of which is soluble in the medium, either coming from serum supplement or secreted by the cells themselves. Ficoll could cause increased adsorption of soluble fibronectin from the medium to the glass surface during extended cell culture. To investigate this, we cultured cells for 2 days with and without Ficoll and, after sample fixation, analyzed antibody-stained fibronectin on the glass surface in areas where the coating was left undisturbed (no apparent harvesting, no cells, no fibers). We switched to antibody staining for fibronectin quantification to ensure that we labeled both cellular and plasma fibronectin, and because this is standard in the field. We also did not add supplemental plasma fibronectin to the medium to correlate with previous studies where this had not been done (data with supplemental fibronectin shown in ESI Fig. 5†). As evident from the images in Fig. 5A, the amount of fibronectin at the surface was increased significantly in the presence of Ficoll. Quantification of the intensity of fibronectin stain showed 2.3× more fibronectin per area on the glass surface in the Ficoll treated condition (Fig. 5B). This means that, though the glass substrates were initially preadsorbed

 

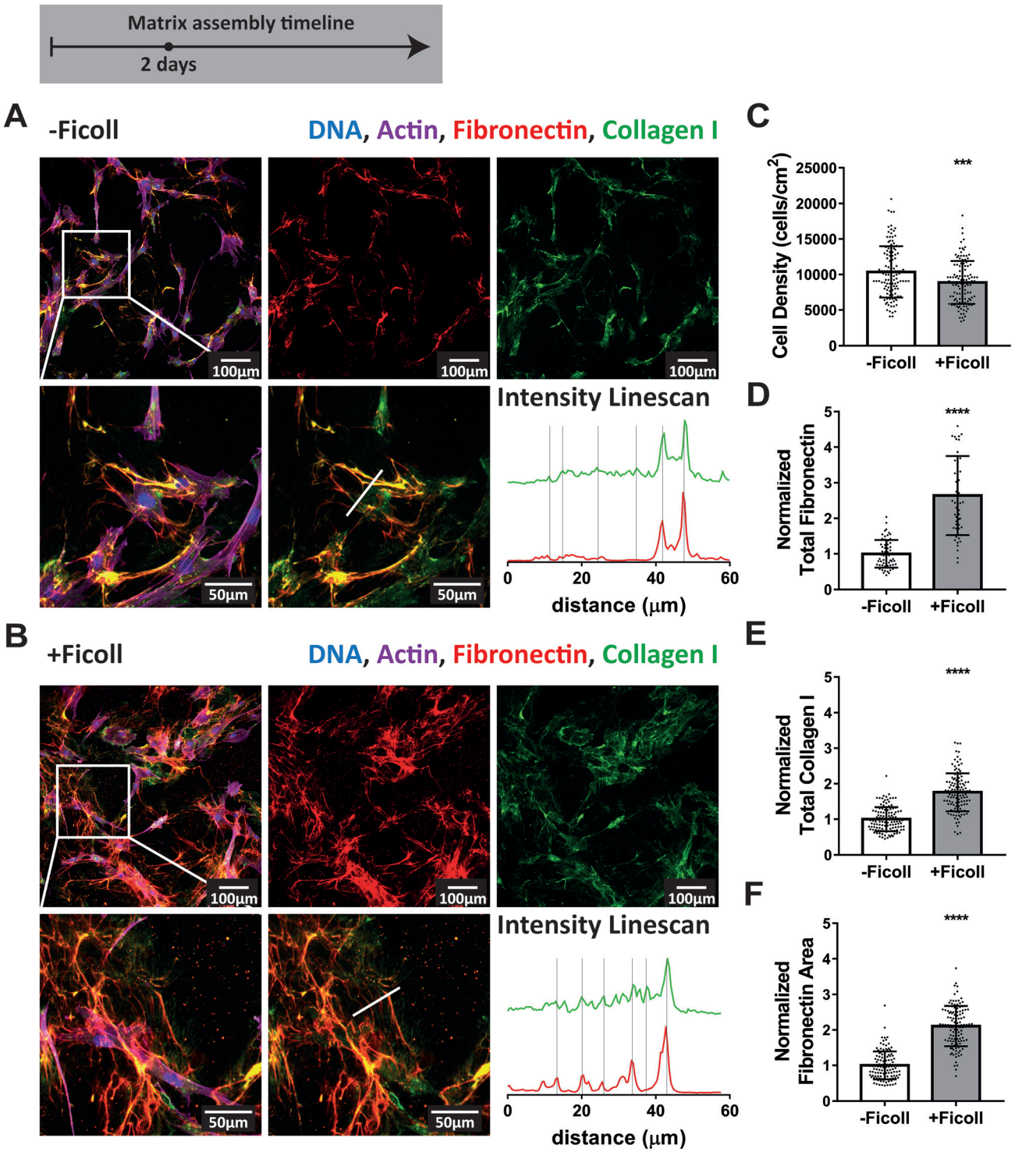


**Fig. 2** Ficoll treatment continues to accelerate assembly of fibronectin and collagen I fibers throughout 2 days and they are still mostly colocalized. (A) ECM assembled without Ficoll. The first row shows a widefield fluorescence image of fibroblasts and matrix followed by images of Alexa-647-labeled fibronectin and antibody-stained collagen I alone. The second row shows a magnified area of the image above, followed by an image of matrix only and intensity linescans of fibronectin and collagen I along the white line indicated in the matrix only image to the left. (B) ECM assembled with Ficoll. (C) Cell density. (D) Summed intensity of Alexa-647-labeled fibronectin. (E) Summed intensity of antibody-stained collagen I. (F) Area of substrate covered by fibronectin fibers as quantified using a threshold set to distinguish fibers from background and coating. 50–120 images were analyzed for each condition. D–F show values normalized to the mean without Ficoll. Glass substrates preadsorbed with 50 μg $mL^{-1}$ plasma fibronectin (10% Alexa-647-labeled). Cells cultured in MEM Alpha supplemented with 10% fetal bovine serum, 1% penicillin–streptomycin, 100 μM L-ascorbic acid 2-phosphate, and 50 μg $mL^{-1}$ plasma fibronectin (10% Alexa-647-labeled). ***indicates $p < 0.001$, ****indicates $p < 0.0001$. Respective greyscale images of each channel can be found in ESI Fig. 2.† ESI Movie 3† shows alternating images of fibronectin and collagen I to appreciate their spatial correlation. Fibronectin matrix quantification by antibody staining can be found in ESI Fig. 4.†

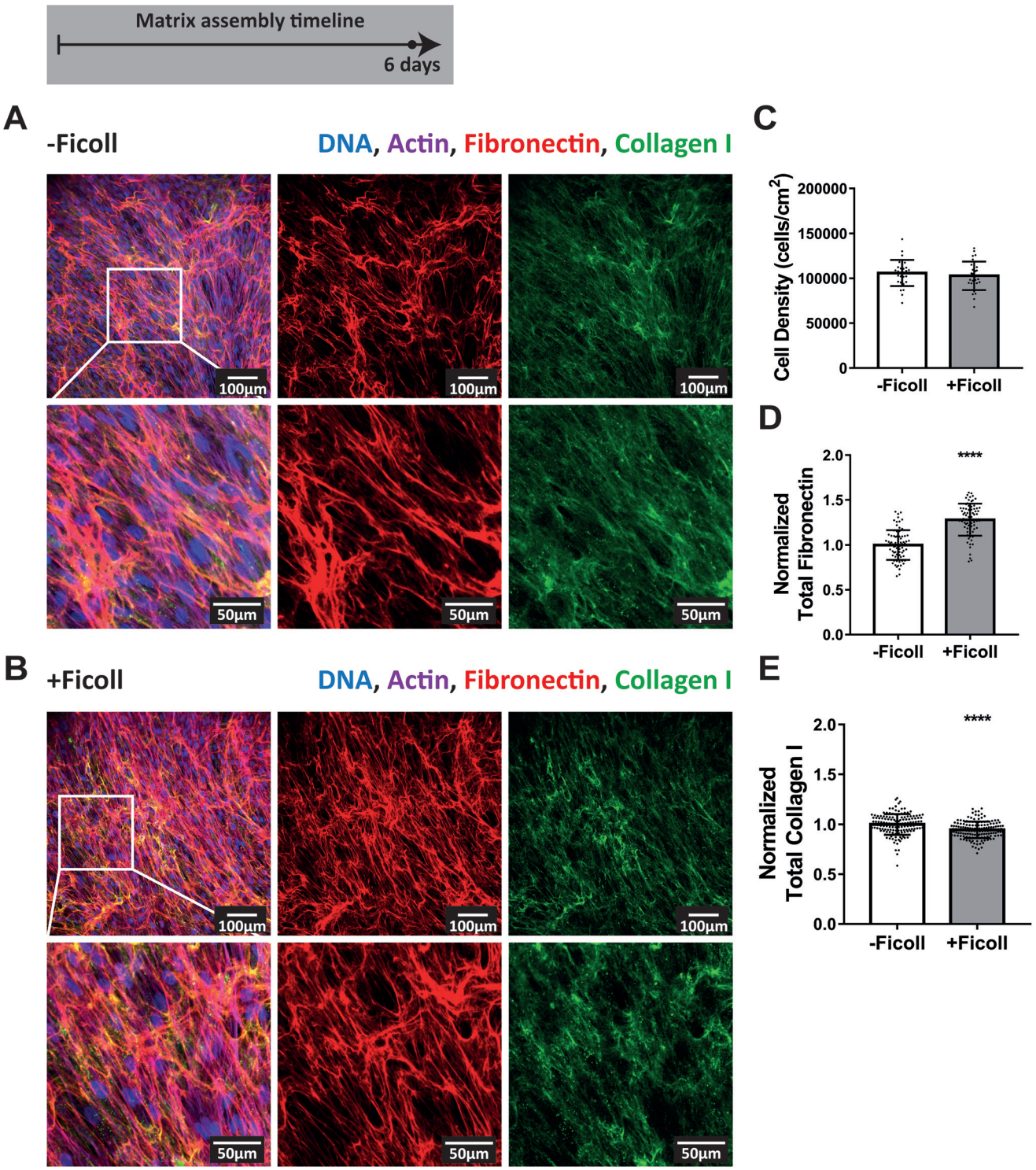


**Fig. 3** ECM assembly after 6 days with and without Ficoll. (A) ECM assembled without Ficoll. The first row shows a widefield fluorescence image of fibroblasts and matrix followed by images of Alexa-647-labeled fibronectin and antibody-stained collagen I alone. The second row shows a magnified area of the image above: first cells and matrix, followed by images of fibronectin and collagen I alone. (B) ECM assembled with Ficoll. (C) Cell density. (D) Summed intensity of Alexa-647-labeled fibronectin. (E) Summed intensity of antibody-stained collagen I. 70–150 images were analyzed for each condition (30 images analyzed for cell density). D and E show values normalized to the mean without Ficoll. Glass substrates preadsorbed with 50 μg $mL^{-1}$ plasma fibronectin (10% Alexa-647-labeled). Cells cultured in MEM Alpha supplemented with 10% fetal bovine serum, 1% penicillin–streptomycin, 100 μM L-ascorbic acid 2-phosphate, and 50 μg $mL^{-1}$ plasma fibronectin (10% Alexa-647-labeled). ****indicates $p < 0.0001$. Respective greyscale images of each channel can be found in ESI Fig. 3.† ESI Movie 4† shows a *z*-stack of 6 day matricies produced with and without Ficoll to appreciate the spatial correlation of fibronectin and collagen I. Fibronectin matrix quantification by antibody staining can be found in ESI Fig. 4.†

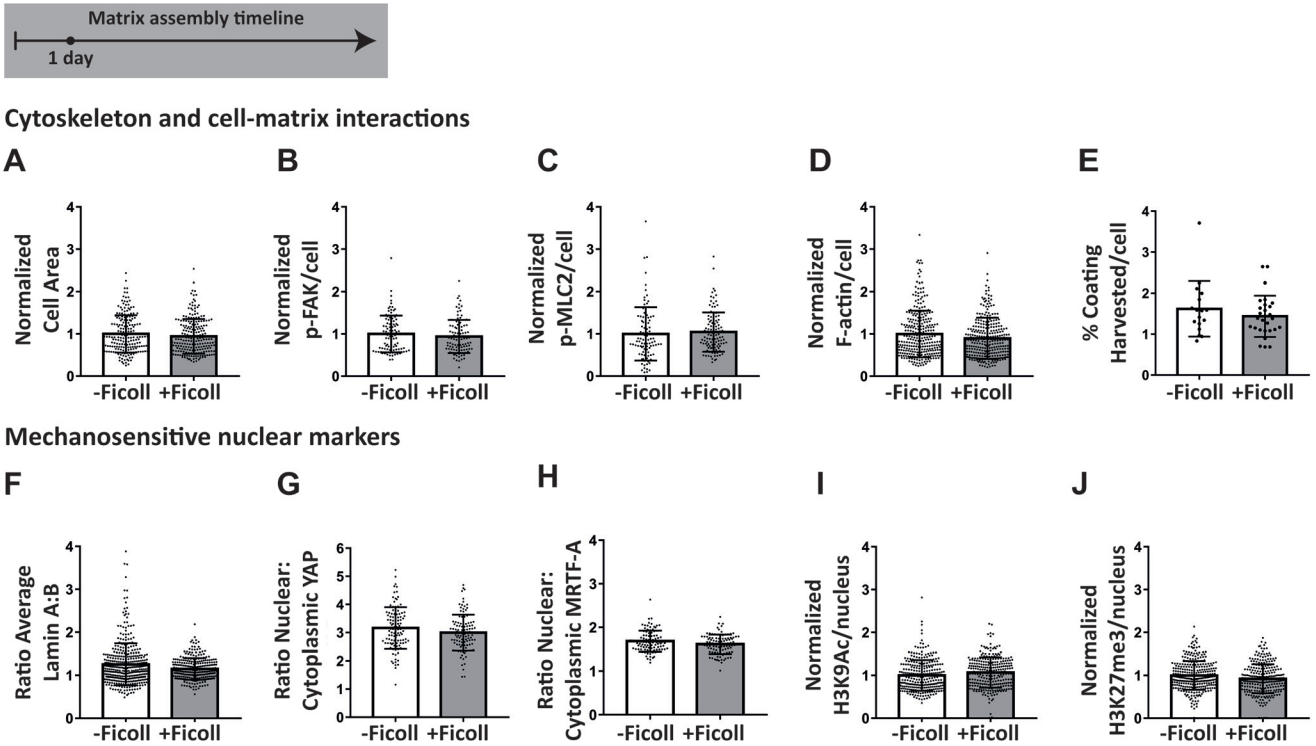


**Fig. 4** Ficoll has no major effect on vital cell mechanical functions. Protein levels were assessed at the single cell level by immunofluorescence microscopy after 24 hours of Ficoll treatment compared to control. (A) Cell area. (B) Summed intensity of phosphorylated focal adhesion kinase per cell. (C) Summed intensity of phosphorylated myosin light chain 2 per cell. (D) Summed intensity of filamentous actin per cell. (E) Percent of image field of view with fibronectin coating removed, divided by the number of cells in the image. Approximately 20 images analyzed per condition. (F) Ratio of average intensity of lamin A to lamin B. (G) Ratio of average intensity of yes-associated protein in the nucleus to the cytoplasm. (H) Ratio of average intensity of myocardin-related transcription factor-A in the nucleus to the cytoplasm. (I) Summed intensity of acetylation of histone 3 at lysine 9 in the nucleus. (J) Summed intensity of trimethylation of histone 3 at lysine 27 in the nucleus. For A–D and F–J, each data point represents one cell. At least 100 individual cells were analyzed per condition. All values except ratios were normalized to the average without Ficoll. Glass substrates preadsorbed with 50 μg $mL^{-1}$ unlabeled plasma fibronectin. Cells cultured in MEM Alpha supplemented with 10% fetal bovine serum, 1% penicillin–streptomycin, and 100 μM L-ascorbic acid 2-phosphate, but no additional plasma fibronectin (aside from that in serum).

with fibronectin, Ficoll treatment caused additional soluble fibronectin from the media to deposit to the glass surface over 2 days of culture.

### With the Ficoll-induced increase in fibronectin matrix there is more un-stretched fibronectin to act as a template for collagen I assembly

Since collagen I assembly is nucleated by binding to low tension rather than highly stretched fibronectin fibers, as fiber stretching destroys the multivalent binding motif by which collagen peptides bind to several fibronectin type I and II modules in a row,[47] similarly to how fiber stretching destroys the binding sites of bacterial adhesins,[68,69] we next asked if Ficoll results in a greater total amount of un-stretched fibronectin fibers that could initiate polymerization of collagen I during the early stages of matrix assembly with our well validated FRET-fibronectin probe.[40,47,51–62] Ten percent of the supplemented plasma fibronectin was FRET-labeled and was incorporated into the matrix assembled by cells, as observed before.[40,54] The glass was preadsorbed with unlabeled fibronectin to distinguish freshly assembled ECM fibers from that adsorbed to the glass substrate. Cell seeding density was doubled (10 000 cells per $cm^2$) to ensure that we had enough fibronectin-FRET signal in an early stage of matrix assembly. Fig. 6A shows representative images of FRET ratios after 2 days, with and without Ficoll. A histogram of all FRET ratios compiled from 21 images for each condition appears in Fig. 6B. The overall peak tensional state of the matrix did not change, which is consistent with our finding that cell contractility did not increase (Fig. 4C). However, the total number of high-FRET pixels was higher upon Ficoll treatment (Fig. 6B). To further assess fibronectin's conformational states, we used different concentrations of the chemical denaturant guanidine hydrochloride (GdnHCl) to gradually denature fibronectin in solution, measured the resulting fibronectin-FRET ratios, and created a calibration curve for our FRET-labeled fibronectin probe, as done before[40,54] (ESI Fig. 6†). Fibronectin in 1 M GdnHCl is extended compared to the globular state in PBS, but has not yet lost its secondary structure, whereas fibronectin in 4 M GdnHCl has lost its secondary structure and is completely denatured.[53] Fibronectin fibrillogenesis is initiated by stretch-induced opening of cryptic fibronectin–fibronectin binding sites[35] and, as cells start bundling fibronectin profilaments into thicker fibers,[70] they can get further stretched up

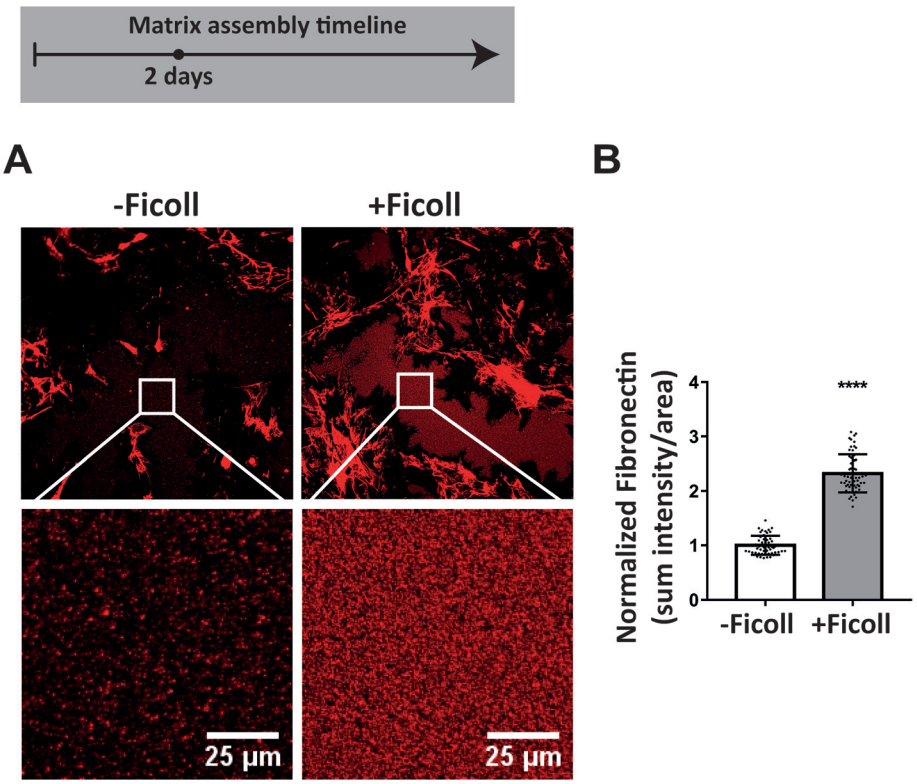


**Fig. 5** Ficoll increases fibronectin adsorption to the glass surface during cell culture. (A) Widefield immunofluorescence images of antibody-stained fibronectin after 2 days culture with and without Ficoll, with insets below showing undisturbed areas of fibronectin coating (no fibroblasts or ECM fibers) that were analyzed. (B) Summed fibronectin intensity divided by area. Glass substrates preadsorbed with 50 μg $mL^{-1}$ unlabeled plasma fibronectin. Cells cultured in MEM Alpha supplemented with 10% fetal bovine serum, 1% penicillin–streptomycin, and 100 μM L-ascorbic acid 2-phosphate, but no additional plasma fibronectin (aside from that in serum). See ESI Fig. 5† for results with plasma fibronectin supplemented to the medium. ****indicates $p < 0.0001$.

to 3–4 times their equilibrium length in cell culture.[56] To quantify the amount of low tension fibronectin, we then quantified the total number of pixels in each image with a FRET ratio above that of fibronectin in 1 M GdnHCl (*i.e.* FRET ratio = 0.34). There was a 30% increase in the amount of low-tension fibronectin with Ficoll at 2 days compared to −Ficoll control (Fig. 6C). Taken together, the overall tensional state of the fibronectin fibers was not changed with Ficoll, but the total number of FRET pixels representing un-stretched fibronectin, and thus potential nucleation sites for collagen I, was significantly higher upon Ficoll treatment.

### Cross-linking adsorbed fibronectin to the substrate inhibits the Ficoll-accelerated matrix assembly

To ask how important surface adsorbed fibronectin might be in the accelerated matrix assembly process as induced by Ficoll, we covalently cross-linked fibronectin to the glass substrate before cell seeding to prevent fibroblasts from scraping off the coating and found that this significantly delayed early assembly of fibronectin fibers. Fig. 7A shows antibody-stained fibronectin and collagen I assembled on a cross-linked fibronectin coating after 2 days. The dark, cell-shaped areas in the fibronectin channel in Fig. 7A are shadows where the fibronectin antibody was not able to access the coating, which we confirmed by removing the cells with trypsin (ESI Fig. 7†). Even though it is known that Ficoll drives the cleavage and assembly of collagen I, we found that Ficoll did not increase collagen I fiber assembly when the fibroblasts could not pull the fibronectin coating off the substrate to accelerate early fibronectin fibrillogenesis (Fig. 7B). In contrast, collagen I fiber assembly was more than doubled by Ficoll on adsorbed fibronectin that the fibroblasts could harvest during the early phase fibrillogenesis (Fig. 7C and D). This is an important novel finding that, even though Ficoll was there to promote the enzymatic cleavage and supramolecular assembly of collagen, the fibronectin fiber template was still essential for collagen I fiber assembly.

### Preadsorbing fibronectin to the glass substrate further accelerates matrix assembly under crowding conditions

To ask how bioengineers can take advantage of our findings, we assessed the impact of preadsorbing fibronectin to the glass substrate on matrix assembly in crowded conditions. We cultured fibroblasts with Ficoll for 2 days on uncoated glass (standard protocol in the community) or glass coated with 50 μg $mL^{-1}$ adsorbed human plasma fibronectin. We found that the cell density was significantly higher when the glass was preadsorbed with fibronectin (Fig. 8A), likely due to both increased cell adhesion and proliferation, and that there

 

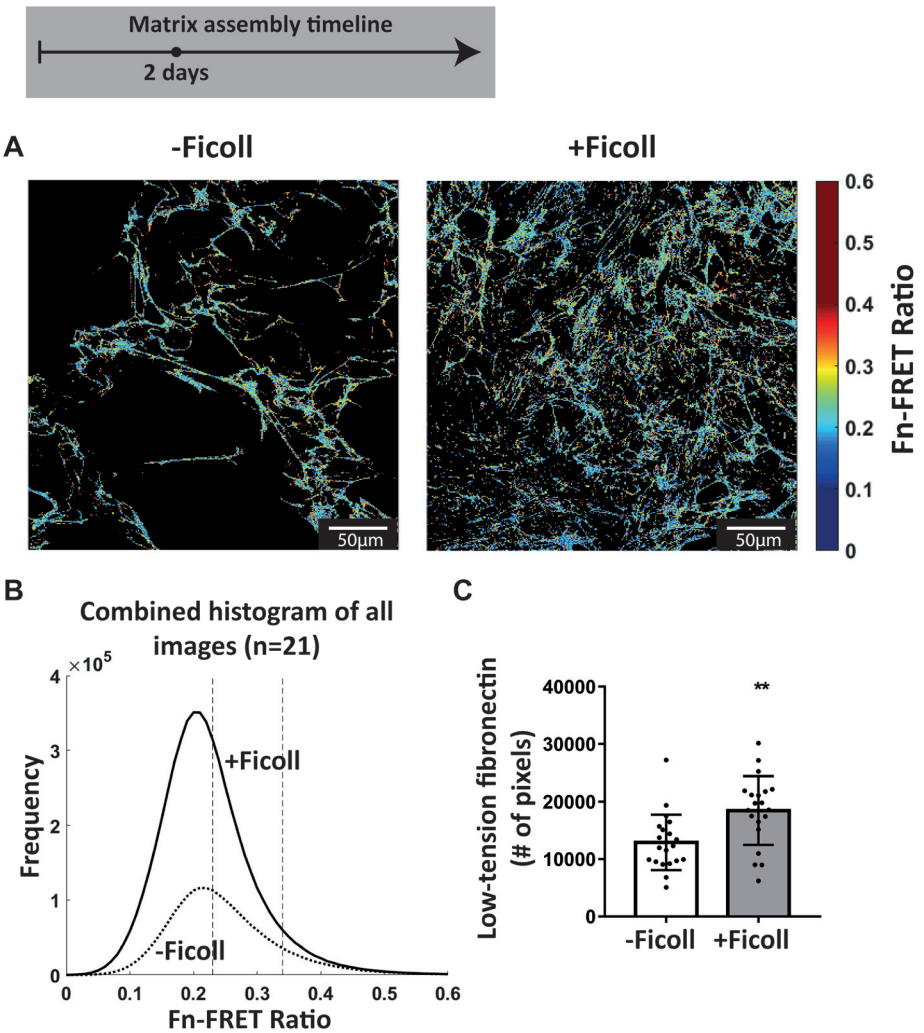


**Fig. 6** Ficoll increases the number of nucleation sites that can induce collagen I polymerization as assessed by fibronectin-FRET, even though the distribution of fibronectin strains is not significantly altered. (A) Confocal images of the fibronectin-FRET ratios at the glass surface (where early matrix fibers are assembled) after 2 days in culture without and with Ficoll. (B) Representative FRET ratio histograms compiled from 21 images for each condition: 7 images each from 3 different samples. The dotted vertical lines represent the average FRET ratios in 4 M GdnHCl (left) and in 1 M GdnHCl (right) – see ESI Fig. 6† for calibration curve. (C) Number of pixels with FRET ratio above that of fibronectin in 1 M GdnHCl. Each point represents a single measurement from one image. Glass substrates preadsorbed with 50 μg $mL^{-1}$ unlabeled plasma fibronectin. Cells cultured in MEM Alpha supplemented with 10% fetal bovine serum, 1% penicillin–streptomycin, 100 μM L-ascorbic acid 2-phosphate, and 50 μg $mL^{-1}$ plasma fibronectin (10% FRET-labeled). **indicates $p < 0.01$.

was much more fibronectin and collagen I fiber assembly than without precoating (Fig. 8B and C). We then added 50 μg $mL^{-1}$ supplemental soluble plasma fibronectin to the medium, in addition to the preadsorbed fibronectin coating, to see if it further improved matrix assembly beyond the coating alone. Note that 10% serum contains only 2–3 μg $mL^{-1}$ of fibronectin.[71] Fig. 8D–F shows that addition of supplemental soluble fibronectin minorly increased cell density but did not impact fibronectin or collagen I assembly. These results show that including fibronectin as a coating before cell seeding markedly improved the matrix assembly with macromolecular crowding in 2 days, but there was no further benefit of also supplementing soluble fibronectin to the medium.

## Discussion and conclusion

Since methods to accelerate matrix production are urgently needed in the fields of tissue engineering and regenerative medicine, our goal here was to shed light on the underpinning mechanisms by which Ficoll exposure upregulates ECM assembly, as previously reported.[11–17,21–23,72,73] Rather than just accelerating pro-collagen cleavage and supramolecular assembly, previously thought to be the main drivers,[2,3] we show here that Ficoll also significantly enhances fibronectin assembly (Fig. 1–3) and that the rate of fibronectin fibrillogenesis regulates the collagen I assembly process. Towards the mechanistic side, we found that fibronectin and collagen I are colocalized during early ECM assembly both with and without

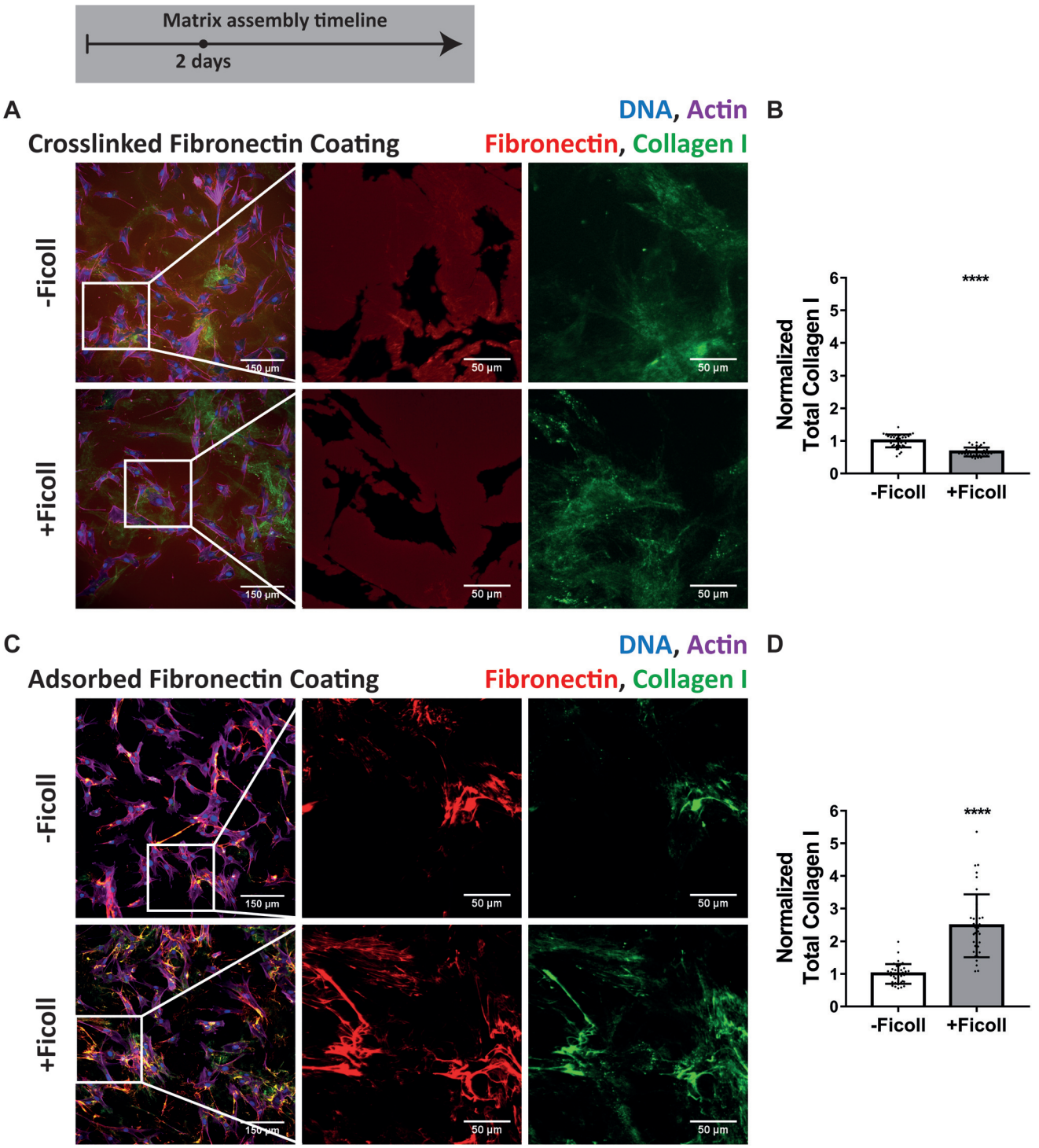


**Fig. 7** Ficoll does not increase collagen I fiber assembly when the preadsorbed fibronectin coating is cross-linked to the substrate prior to cell seeding. (A) Widefield immunofluorescence images of matrix assembled on cross-linked fibronectin coating (50 μg mL$^{-1}$, unlabeled) after 2 days of culture. The first image is of fibroblasts and matrix, followed by magnified images of fibronectin and collagen I alone. Dark areas in the fibronectin channel are cell shadows, not harvested coating – see ESI Fig. 7† for confirmation. (B) Summed intensity of collagen I, normalized to the mean without Ficoll. (C and D) Same for adsorbed fibronectin coating (50 μg mL$^{-1}$, unlabeled). Cells cultured in MEM Alpha supplemented with 10% fetal bovine serum, 1% penicillin–streptomycin, and 100 μM L-ascorbic acid 2 phosphate, but no additional plasma fibronectin (aside from that in serum). ****indicates $p < 0.0001$. ESI Movie 1† shows how cells are able to harvest an adsorbed fibronectin coating, which is inhibited by cross-linking of fibronectin to the glass.

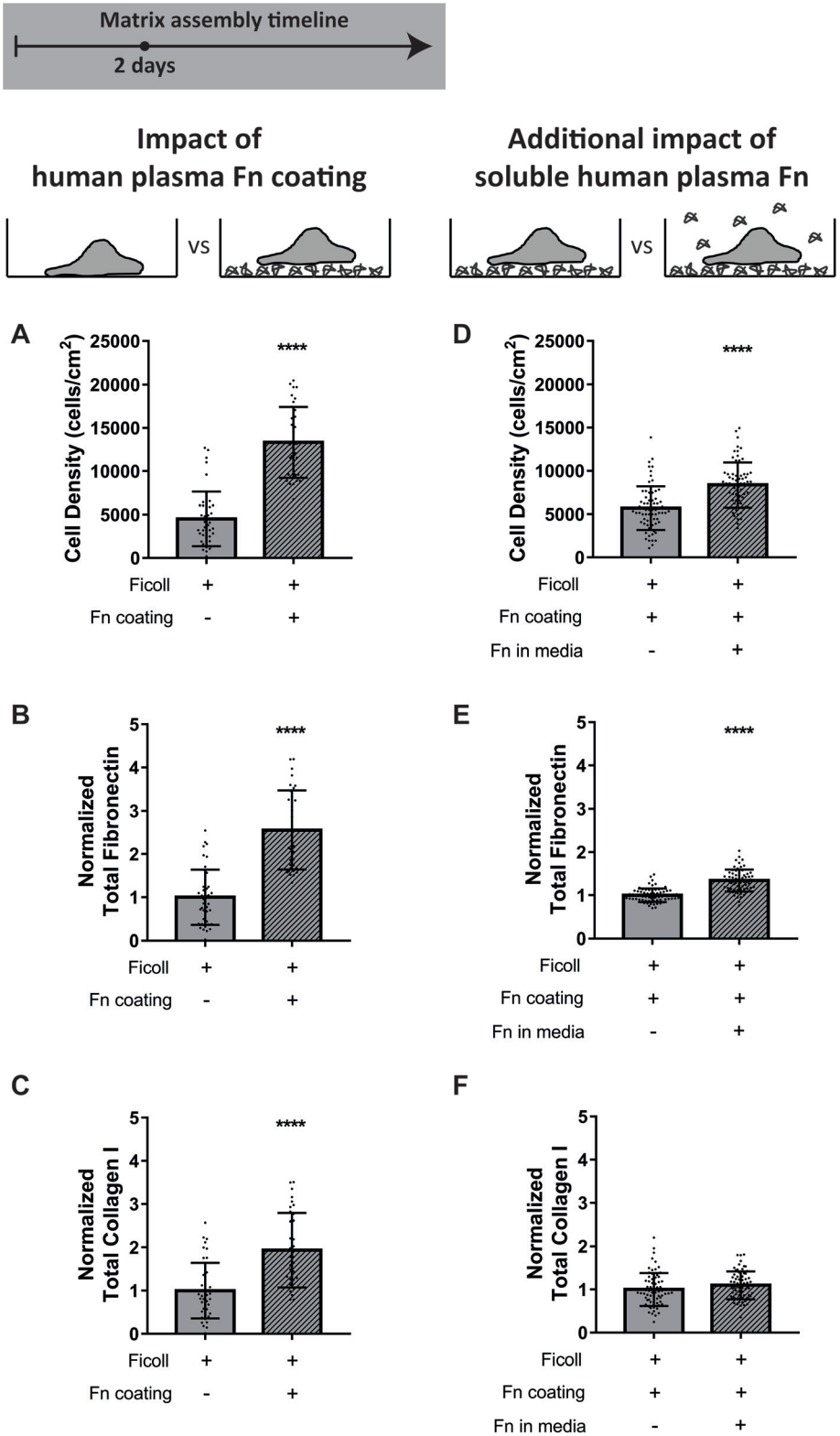


**Fig. 8** Supplementation of fibronectin as an adsorbed coating improves matrix assembly in the presence of Ficoll after 2 days. (A–C) Tissue production in the presence of Ficoll on uncoated glass compared to glass coated with 50 μg $mL^{-1}$ adsorbed human plasma fibronectin (unlabeled). (A) Cell density. (B) Summed intensity of antibody-stained fibronectin. (C) Summed intensity of antibody-stained collagen I. B and C are normalized to the mean value on uncoated glass. (D–F) Additional impact of adding 50 μg $mL^{-1}$ soluble human plasma fibronectin (unlabeled) when there is already an adsorbed fibronectin coating. Cells cultured in MEM Alpha supplemented with 10% fetal bovine serum, 1% penicillin–streptomycin, and 100 μM L-ascorbic acid 2 phosphate. ****indicates $p < 0.0001$.

crowders (Fig. 1–3, ESI Movies 2–4†), and that even though the cell mechanical functions are not significantly impacted (Fig. 4), Ficoll causes a significant increase in soluble fibronectin adsorbing from the medium to the substrate surface (Fig. 5 and ESI Fig. 5†). We observed a high density of bright fibronectin spots at the glass surface, but only in the presence of Ficoll (Fig. 1–2 and ESI Fig. 5†), suggesting that crowding causes aggregation of fibronectin, which likely contributes to further increasing the amount of fibronectin that the cells can harvest. The 2-fold increase in fibronectin at the glass surface seen with Ficoll correlates well with the 2-fold increase in early fibronectin fiber assembly (Fig. 1–2). Even though the cell spreading area and the area of coating harvested per cell are not significantly affected by Ficoll (Fig. 4), there is a significantly higher amount of fibronectin on the surface which the fibroblasts can scrape off. Fibronectin harvesting from the substrate is much more effective than from the medium because surface adsorbed fibronectin is in a more open conformation with greater accessibility of cell-binding sites than fibronectin in solution.[53,74] Additionally, fibroblasts can more readily exert tensional forces on surface-bound than on freely floating fibronectin, which is important since cells have to stretch fibronectin to induce its fibrillogenesis.[35,39,70]

By exploiting our well-established fibronectin-FRET probe,[40,47,51–62] we could show that Ficoll significantly increases the total amount of low-tension fibronectin fibers (Fig. 6). This observation is highly significant since we showed previously that fibronectin stretching destroys the multivalent binding motif for the collagen peptide,[35,47] and consequently, only the low-tension fibronectin fibers can nucleate the initial collagen I polymerization process in cell culture. A very recent study showed that fibronectin also binds both procollagen and the C-proteinase BMP-1, thereby acting as a template to increase their interaction.[49] This suggests that the increase in fibronectin matrix with crowding could directly contribute to enhanced cleavage of procollagen, implicating yet another role for fibronectin in matrix assembly with crowding.

Since the rate by which fibronectin can be scraped off plays a key role in Ficoll-enhanced ECM assembly, we next asked whether chemical cross-linking to the substrate might slow the matrix assembly rate. Indeed we found that crosslinking of the pre-adsorbed fibronectin layer to the substrate abolished the previously described ability of Ficoll to upregulate matrix assembly (Fig. 7). This is a remarkable finding since it was shown previously that Ficoll upregulates procollagen cleavage and supramolecular assembly,[1,2,20,21,27–31] and still, if the cells cannot efficiently harvest surface bound fibronectin to build fibers, Ficoll does not upregulate ECM assembly. We thus illuminate for the first time the essential role of fibronectin in the underpinning mechanism by which Ficoll upregulates ECM assembly.

But what can tissue engineers learn from having deeper insights into the driving mechanism? Our finding that cross-linking of fibronectin to the glass surface also prevents collagen assembly, even in the presence of a neutral crowder (Fig. 7), demonstrates that paying attention solely to the crowder is not enough to catalyze collagen assembly *in vitro*. While it is common among tissue engineers to expose their materials to the medium before cell seeding, we show here that preadsorbing human plasma fibronectin greatly accelerates ECM production compared to the uncoated sample (Fig. 8) and that crosslinking of the preadsorbed fibronectin layer to the substrates destroys the accelerating effect of Ficoll supplementation (Fig. 7). We found that after 6 days there is no longer a large difference in the matrix assembled with and without Ficoll (Fig. 3 and ESI Fig. 4†). Results in the literature are mixed about whether the increased matrix with crowding persists over long culture times or if the matrix assembly without crowding eventually catches up[11,15,17,24,26] (summarized in ESI Table 2†). However, there seems to be a consensus that crowding increases the speed of early matrix assembly, as we too have shown (Fig. 1 and 2). This increase in speed in the early phases is highly valuable in tissue engineering, where the weeks to months traditionally needed to produce a substitute tissue *in vitro* result in high costs, a long wait-time for the patient, and changes in cell phenotype, limiting clinical success.

As tissue engineers move away from the use of standard fetal bovine serum towards animal-free media,[73] it will become even more important to consider whether to supplement the media with fibronectin and at what concentrations. As we have shown here, it is highly beneficial to supplement purified human plasma fibronectin in the form of an adsorbed coating (Fig. 8). This may be even more impactful in cases where the cells do not efficiently produce fibronectin on their own. Our mechanistic insights give tissue engineers important new parameters to consider which can be tuned to effectively increase the ECM assembly process.

## Materials and methods

### Isolation of human plasma fibronectin

Fibronectin was isolated from human plasma as described previously,[54] with minor modifications. First, plasma (Blood Bank Zurich, Switzerland) was spun at 3220*g* for 40 minutes at 8 °C. 10 mM EDTA was added to the supernatant and then the supernatant was passed through a PD-10 desalting column (GE Healthcare #17-0851-01). Next the supernatant was passed through a poly-prep chromatography column (Bio-Rad #7311550) pre-packed the day before with gelatin-sepharose 4B (VWR #17-0956-01) to bind fibronectin. The column was then washed with column buffer (PBS + 10 mM EDTA), followed by 1 M NaCl in column buffer, and 0.2 M Arginine (Carl Roth #1655) in column buffer until the 280 nm absorbance of the flow-through was <0.1. Finally, the fibronectin was eluted with 1 M arginine in column buffer and stored at −80 °C until usage. The quality of fibronectin purification was confirmed by western blot and Coomassie staining. Before usage in cell culture, fibronectin was slowly thawed at 4 °C overnight and the solvent was changed to PBS through dialysis with a Slide-A-Lyzer Dialysis Cassette (ThermoFischer Scientific #66003).

 

### Substrate cleaning and fibronectin preadsorption

Glass coverslips were cleaned by soaking in 2% HellmaneX solution (Hellma #9-307-010-507) with sonication for 30 minutes, followed by another 30 minutes without sonication, and subsequently washed with deionized water and blown dry. Coverslips were then coated by adsorbing human plasma fibronectin from solution (50 μg $mL^{-1}$ in PBS, 1 hour, room temperature) and subsequently washed with PBS. Coverslips were sterilized before cell culture by 15 minutes of UV exposure in a biosafety cabinet.

### Cell culture

Normal human dermal fibroblasts (PromoCell, Vitaris AG, Switzerland) were cultured in standard medium consisting of MEM Alpha (Biowest #L0475), 10% fetal bovine serum (Biowest #S181H), and 1% penicillin–streptomycin (Gibco #15140122). Fibroblasts were regularly passaged with 0.25% Trypsin-EDTA (Invitrogen #25200-056) before reaching confluence and used at passage #6-9. Medium with crowders was prepared by dissolving 37.5 mg $mL^{-1}$ of 70 kDa Ficoll (GE Healthcare #GE17-0310) and 25 mg $mL^{-1}$ of 400 kDa Ficoll (GE Healthcare #GE17-0300) in standard medium in a 37 °C water bath. Once dissolved, Ficoll containing medium was filtered through a 0.22 μm syringe filter. Standard medium with no crowder was also filtered for control samples. This crowding formulation remained consistent throughout the study.

### Extracellular matrix assembly

For ECM assembly experiments, fibroblasts were cultured on coverslips coated with adsorbed fibronectin placed inside standard 12-well polystyrene tissue culture plates. After coating, coverslips were washed with PBS and fibroblasts were plated in standard medium at 5000 cells per $cm^2$ and allowed to adhere for 1 hour in a humidified incubator with 5% $CO_2$. Afterwards, media were changed to ±Ficoll as appropriate and supplemented with 100 μM L-ascorbic acid 2-phosphate (Sigma #A8960) and 50 μg $mL^{-1}$ human plasma fibronectin purified in house (see Methods section "Isolation of human plasma fibronectin"). Fibroblasts were cultured for 16 hours, 2 days, or 6 days. Media were changed after 3 days for the 6-day samples. Ascorbic acid and fibronectin were freshly added upon media change.

### Immunofluorescence and microscopy

ECM assembly was visualized by immunofluorescence microscopy. Unless labeled-fibronectin was used, fibronectin was stained with BD primary antibody #610077 (1 : 200) and donkey anti-mouse-488 secondary antibody (Invitrogen #A-21202, 1 : 200). Collagen was visualized with Abcam primary antibody #34710 (1 : 200) and donkey anti-rabbit-546 secondary antibody (Invitrogen #A10040, 1 : 200). Actin was visualized with Phalloidin 647 or 488 (Invitrogen, 1 : 500) and DNA with Hoechst 33342 (Thermo Scientific #62249, 1 : 200). Samples were first blocked in 5% w/v BSA (AppliChem GmbH #A1391) in water for 1 hour, then incubated with primary antibody in 5% BSA for 1 hour at room temperature, followed by washing with 1% BSA and incubation with secondary antibody in 5% BSA for 1 hour at room temperature. Samples were then permeabilized with 0.3% Triton X-100 (AppliChem #A4975) for 15 minutes, washed, and stained with actin and DNA dyes. Samples were finally mounted with fluorescent mounting medium (Dako #S3023) and allowed to dry overnight at room temperature before imaging.

Phosphorylated FAK was immunolabeled with Abcam primary antibody #81298 (1 : 400) and phosphorylated myosin light chain 2 was immunolabeled with Cell Signaling Technologies primary antibody #3671 (1 : 50). Both were visualized with donkey anti-rabbit-546 secondary antibody (Invitrogen #A10040, 1 : 200). MRTF-A was immunolabeled with Abcam primary antibody #49311 (1 : 100), H3K9Ac with Abcam primary antibody #4441 (1 : 150), and H3K27me3 with Cell Signaling Technologies primary antibody #9733 (1 : 1600). Each of these were then visualized in individual samples with goat anti-rabbit 488 secondary antibody #A-11034 (1 : 200). Lamin A and lamin B were co-stained with primary antibodies ab8980 (Abcam, 1 : 200) and ab16048 (Abcam, 1 : 500) and secondary antibodies donkey anti-mouse 488 (Invitrogen #A-21202, 1 : 200) and donkey anti-rabbit 546 (Invitrogen #A10040), respectively. Staining proceeded as above, except permeabilization occurred just after fixing and before primary and secondary antibody incubations.

Images for quantification of ECM assembly and cell/nuclear markers were taken on a Leica DMI6000B epifluorescence microscope with 20× 0.7NA HC PlanApo objective. A mosaic of 20 images (5 × 4 grid) was captured to avoid bias in selecting areas to image. An ROI was selected to avoid corners where fluorescent lamp intensity was weaker. Some images were also taken with a Leica SP5 confocal microscope to better visualize small details and appreciate the dimensionality of the matrix.

### Labeling of fibronectin

Unless specified otherwise, fibronectin matrix assembly was visualized by substituting 10% of the coating and supplemented soluble fibronectin with fluorescently-labeled fibronectin (5 μg $mL^{-1}$ labeled + 45 μg $mL^{-1}$ unlabeled). Fibronectin was randomly labeled with fluorescent probes on surface accessible lysine residues by amide bond formation, as described before[70] with minor modifications. After purification of fibronectin, the solvent was changed from 1 M arginine to labelling buffer (0.1 M $NaHCO_3$ in PBS, pH 8.5) through dialysis with a Slide-A-Lyzer Dialysis Cassette (ThermoFischer Scientific #66003). Fibronectin in the dialysis cassette was then incubated with a molar excess of Alexa Fluor 647 succinimidyl ester (Invitrogen #A20006). The molar excess depended on the freshness of the dye and varied from 5–50 (lower values for more fresh dye). Fibronectin was then dialyzed again to change the solvent to PBS.

For FRET measurements, fibronectin was randomly labeled with Alexa 488 donor fluorophores on its amines *via* succinimidyl ester conjugation and specifically labeled with Alexa 546

acceptor fluorophores on the cysteines in fibronectin type III modules $FNIII_7$ and $FNIII_{15}$ *via* maleimide conjugation, based on previous protocols[52,54,56] and as described by Ortiz Franyuti *et al.*[62] To validate successful labeling, the sensitivity of the FRET-probe to progressive denaturation in increasing concentrations of guanidine hydrochloride (GdnHCl, Sigma #G4505) was verified with a procedure slightly modified from what was described previously.[54] A coverslip was coated with 2% BSA for 30 minutes, then washed with distilled water and blown dry. FRET-labeled fibronectin was dissolved in solutions of GdnHCl ranging from 4 M to 0 M ($dH_2O$ control). A 2.5 μL drop of each solution was placed on the coverslip and was imaged in 5 ROIs above the glass-droplet interface with the same microscope settings as used for the matrices (see Methods section "Imaging of FRET in cell-assembled matrices"). Average FRET ratios were calculated for each concentration and plotted as a denaturation curve.

### Quantification of ECM and cell density

ECM assembly was quantified by summing fibronectin and collagen intensity per image after background subtraction with a custom MATLAB script. Cell density was quantified by automated segmentation of nuclei with a custom MATLAB script for 16 hours and 2 day samples. 6 day samples were counted manually because the density was too high for automatic segmentation.

### Quantification of fibronectin adsorbed to the glass surface

Fibroblasts were cultured on fibronectin coated glass as described above, except without soluble fibronectin added to the media. After 2 days, samples were fixed, stained, and imaged as described above. The amount of fibronectin on the surface was quantified by measuring the fluorescence intensity in an area where the fibronectin layer looked uniform and there were no cells or matrix fibers. The summed intensity was divided by the area of the ROI and reported as fibronectin density. One ROI per image was analyzed. Some images showed abnormally high fluorescence intensity at the glass surface. This could be due to autofluorescence from HellmaneX solution that was not fully washed. These images with abnormal coating were identified by viewing all images simultaneously and they were excluded from the analysis.

### Quantification of cell/nuclear markers and percentage of coating harvested

Cell areas were estimated by manual tracing. Intensity of F-actin, p-FAK, and p-MLC2 per cell were summed in the manually traced cell outline after background subtraction. Only spread cells with few cell–cell contacts were analyzed. The percentage of the coating harvested per cell was measured by setting a threshold to distinguish the intact coating and fibronectin fibers from areas of the glass where the coating had been removed (darker areas). The area below the threshold was measured and divided by the total area to get the percentage of the coating that was harvested. This value was then divided by the number of cells identified by automatic segmentation of the nuclei. YAP and MRTF-A nuclear-to-cytoplasmic ratios were measured manually in ImageJ software. Lamin A, Lamin B, H3K9Ac, and H3K27me3 were quantified by automatic nuclear segmentation in MATLAB.

### Matrix assembly with FRET-labeled fibronectin

Fibroblasts were cultured in glass bottom Lab-tek chambers (Thermo Fisher Scientific #155411) that had been previously coated with unlabeled fibronectin (as described above). Cells were plated at 10 000 cells per $cm^2$ to achieve greater matrix assembly and ensure that there was enough signal to analyze FRET. After 1 hour cell adhesion, media were changed to ±Ficoll and supplemented with 100 μM L-ascorbic acid 2-phosphate, 45 μg $mL^{-1}$ unlabeled fibronectin, and 5 μg $mL^{-1}$ FRET-labeled fibronectin. Cells were cultured for 2 days, then washed with PBS and fixed with 4% PFA for 20 minutes.

### Imaging of FRET in cell-assembled matrices

Samples were imaged in PBS immediately after fixation with an Olympus FV1000 confocal microscope with a 40× water immersion objective. Samples were excited with a 488 nm laser and both the donor and acceptor emission were collected simultaneously. Two day old matrices were imaged in one focal plane where a majority of the matrix, particularly the smallest fibers, were in focus. A Kalman line filter was applied as a software setting at the time of image acquisition.

### Analysis of FRET in cell-assembled matrices

Images of FRET labeled fibronectin were analyzed with custom MATLAB code as described previously.[54] Briefly, dark current background from the detector was subtracted from both the donor and acceptor images. Next, images were smoothed with a 2 × 2 pixel averaging filter. A threshold was applied to exclude low intensity signal from the fibronectin coating and background (selecting only for fibronectin fibers), as well as any saturated pixels. Then bleedthrough from the donor channel into the acceptor channel was corrected for by subtracting 20% of the donor image from the acceptor image, pixel-by-pixel. Finally, FRET ratios were calculated by dividing the pixel intensities of the acceptor image by the donor image.

### Cross-linking fibronectin to the coverslip

For cross-linked fibronectin coating, coverslips were first plasma treated (Harrick Plasma PDC-32G) for 30 seconds at maximum power. Coverslips were then incubated for 15 minutes with 2% (3-aminopropyl)triethoxysilane (Sigma-Aldrich #A3648) solution in DI water (made fresh). After rinsing with DI water, coverslips were treated with 0.125% glutaraldehyde (Sigma-Aldrich #G4004) in water for 30 minutes. Coverslips were washed again and coated with 50 μg $mL^{-1}$ fibronectin in PBS for 1 hour. After washing with PBS, coverslips were sterilized with UV for 15 minutes before cell plating. Cell culture proceeded as described above. Ascorbic acid was supplemented to the media, but not plasma fibronectin.

### Statistical analysis

Unpaired, parametric *t*-tests were performed with GraphPad Prism software to test for statistical significance. *P*-Values relative to control are indicated by stars in figures and defined in figure captions.

## Conflicts of interest

There are no conflicts of interest to declare.

## Acknowledgements

Financial support from ETH Zürich, the Institute for International Education (Whitaker International Program Fellowship, Jenna Graham), and the National Cancer Institute at the National Institutes of Health (Grant #U54CA210173, Denis Wirtz) are greatly appreciated. The authors would also like to thank Dr Denis Wirtz for invaluable support and useful discussions, Dr Jens Möller for many valuable discussions and helpful input, Chantel Spencer for isolating human plasma fibronectin, Sebastian Lickert and Kateryna Selcuk for providing fluorescently-labeled fibronectin, Mario Benn for help with FRET experiments and for providing FRET-labeled fibronectin, Dr Simon Arnoldini for providing the code for FRET analysis, Dr Nikhil Jain for help getting this project started, and Charlotte Fonta for help reviewing this manuscript. Support was also provided by Justine Kusch and the ScopeM microscopy center at ETH.

## References

1 J. F. Bateman, W. G. Cole, J. J. Pillow and J. A. Ramshaw, Induction of procollagen processing in fibroblast cultures by neutral polymers, *J. Biol. Chem.*, 1986, **261**(9), 4198–4203.
2 C. Chen, F. Loe, A. Blocki, Y. Peng and M. Raghunath, Applying macromolecular crowding to enhance extracellular matrix deposition and its remodeling in vitro for tissue engineering and cell-based therapies, *Adv. Drug Delivery Rev.*, 2011, **63**(4–5), 277–290.
3 P. Benny and M. Raghunath, Making microenvironments: A look into incorporating macromolecular crowding into in vitro experiments, to generate biomimetic microenvironments which are capable of directing cell function for tissue engineering applications, *J. Tissue Eng.*, 2017, **8**, 2041731417730467.
4 R. J. Ellis, Macromolecular crowding: obvious but underappreciated, *Trends Biochem. Sci.*, 2001, **26**(10), 597–604.
5 M. A. Mourão, J. B. Hakim and S. Schnell, Connecting the Dots: The Effects of Macromolecular Crowding on Cell, *Biophys. J.*, 2014, **107**(12), 2761–2766.
6 S. B. Zimmerman and A. P. Minton, Macromolecular Crowding: Biochemical, Biophysical, and Physiological Consequences, *Annu. Rev. Biophys. Biomol. Struct.*, 1993, **22**(1), 27–65.
7 N. A. Chebotareva, B. I. Kurganov and N. B. Livanova, Biochemical effects of molecular crowding, *Biochemistry*, 2004, **69**(11), 1239–1251.
8 M. Weiss, Crowding, diffusion, and biochemical reactions, *Int. Rev. Cell Mol. Biol.*, 2014, **307**, 383–417.
9 I. M. Kuznetsova, K. K. Turoverov and V. N. Uversky, What macromolecular crowding can do to a protein, *Int. J. Mol. Sci.*, 2014, **15**(12), 23090–23140.
10 G. Rivas and A. P. Minton, Macromolecular Crowding In Vitro, In Vivo, and In Between, *Trends Biochem. Sci.*, 2016, **41**(11), 970–981.
11 R. Rashid, N. S. J. Lim, S. M. L. Chee, S. N. Png, T. Wohland and M. Raghunath, Novel Use for Polyvinylpyrrolidone as a Macromolecular Crowder for Enhanced Extracellular Matrix Deposition and Cell Proliferation, *Tissue Eng., Part C*, 2014, **20**(12), 994–1002.
12 A. S. Zeiger, F. C. Loe, R. Li, M. Raghunath and K. J. Van Vliet, Macromolecular crowding directs extracellular matrix organization and mesenchymal stem cell behavior, *PLoS One*, 2012, **7**(5), e37904.
13 F. D. Liu, A. S. Zeiger and K. J. Van Vliet, Time-Dependent Extracellular Matrix Organization and Secretion from Vascular Endothelial Cells due to Macromolecular Crowding, *MRS Online Proc. Libr.*, 2014, **1623**, mrsf13-1623-f02-10.
14 X. M. Ang, M. H. C. Lee, A. Blocki, C. Chen, L. L. S. Ong, H. H. Asada, *et al.*, Macromolecular crowding amplifies adipogenesis of human bone marrow-derived mesenchymal stem cells by enhancing the pro-adipogenic microenvironment, *Tissue Eng., Part A*, 2014, **20**(5–6), 966–981.
15 P. Kumar, A. Satyam, X. Fan, E. Collin, Y. Rochev, B. J. Rodriguez, *et al.*, Macromolecularly crowded in vitro microenvironments accelerate the production of extracellular matrix-rich supramolecular assemblies, *Sci. Rep.*, 2015, **5**(1), 8729.
16 P. Benny, C. Badowski, E. B. Lane and M. Raghunath, Making More Matrix: Enhancing the Deposition of Dermal–Epidermal Junction Components In Vitro and Accelerating Organotypic Skin Culture Development, Using Macromolecular Crowding, *Tissue Eng., Part A*, 2015, **21**(1–2), 183–192.
17 M. C. Prewitz, A. Stißel, J. Friedrichs, N. Träber, S. Vogler, M. Bornhäuser, *et al.*, Extracellular matrix deposition of bone marrow stroma enhanced by macromolecular crowding, *Biomaterials*, 2015, **73**, 60–69.
18 M. Harada, N. Aoyagi, K. Kondo, C. Ishino, K. Odaka, K. Matsue, *et al.*, Allogeneic bone marrow transplantation from a major ABO-incompatible donor. Infusion of hemopoietic stem cells isolated by Ficoll-Hypaque method, *Transplantation*, 1983, **35**(2), 191–192.
19 A. N. Laessker, T. Hardarsson, A.-S. Forsberg, T. Mukaida and P. V. Holmes, Appendix G: Vitrification of Blastocysts Using VitriBlastTM and ThermoBlastTM: Nidacon, in

*Cryopreservation of Mammalian Gametes and Embryos Methods in Molecular Biology*, ed. Z. Nagy, A. Varghese and A. Agarwal, Humana Press, New York, NY, 1568th ed, 2017, pp. 355–365.

20 C. Z. Chen, Y. X. Peng, Z. B. Wang, P. V. Fish, J. L. Kaar, R. R. Koepsel, *et al.*, The Scar-in-a-Jar: studying potential antifibrotic compounds from the epigenetic to extracellular level in a single well, *Br. J. Pharmacol.*, 2009, **158**(5), 1196–1209.

21 Y. Peng and M. Raghunath, Learning From Nature: Emulating Macromolecular Crowding To Drive Extracellular Matrix Enhancement For The Creation Of Connective Tissue in vitro, in *Tissue Engineering*, ed. D. Eberli, IntechOpen, 2010.

22 A. Satyam, P. Kumar, X. Fan, A. Gorelov, Y. Rochev, L. Joshi, *et al.*, Macromolecular crowding meets tissue engineering by self-assembly: a paradigm shift in regenerative medicine, *Adv. Mater.*, 2014, **26**(19), 3024–3034.

23 M. Graupp, H.-J. Gruber, G. Weiss, K. Kiesler, S. Bachna-Rotter, G. Friedrich, *et al.*, Establishing principles of macromolecular crowding for in vitro fibrosis research of the vocal fold lamina propria, *Laryngoscope*, 2015, **125**(6), E203–E209.

24 D. Cigognini, D. Gaspar, P. Kumar, A. Satyam, S. Alagesan, C. Sanz-Nogués, *et al.*, Macromolecular crowding meets oxygen tension in human mesenchymal stem cell culture - A step closer to physiologically relevant in vitro organogenesis, *Sci. Rep.*, 2016, **6**, 30746.

25 P. Kumar, A. Satyam, D. Cigognini, A. Pandit and D. I. Zeugolis, Low oxygen tension and macromolecular crowding accelerate extracellular matrix deposition in human corneal fibroblast culture, *J. Tissue Eng. Regener. Med.*, 2017, 6–18.

26 D. Gaspar, K. P. Fuller and D. I. Zeugolis, Polydispersity and negative charge are key modulators of extracellular matrix deposition under macromolecular crowding conditions, *Acta Biomater.*, 2019, **88**, 197–210.

27 Y. Hojima, B. Behta, A. M. Romanic and D. J. Prockop, Cleavage of Type I Procollagen by C- and N-Proteinases Is More Rapid If the Substrate Is Aggregated with Dextran Sulfate or Polyethylene Glycol, *Anal. Biochem.*, 1994, **223**(2), 173–180.

28 R. R. Lareu, K. H. Subramhanya, Y. Peng, P. Benny, C. Chen, Z. Wang, *et al.*, Collagen matrix deposition is dramatically enhanced in vitro when crowded with charged macromolecules: The biological relevance of the excluded volume effect, *FEBS Lett.*, 2007, **581**(14), 2709–2714.

29 R. R. Lareu, I. Arsianti, H. K. Subramhanya, P. Yanxian and M. Raghunath, In vitro enhancement of collagen matrix formation and crosslinking for applications in tissue engineering: a preliminary study, *Tissue Eng.*, 2007, **13**(2), 385–391.

30 J.-Y. Dewavrin, N. Hamzavi, V. P. W. Shim and M. Raghunath, Tuning the architecture of three-dimensional collagen hydrogels by physiological macromolecular crowding, *Acta Biomater.*, 2014, **10**(10), 4351–4359.

31 J.-Y. Dewavrin, M. Abdurrahiem, A. Blocki, M. Musib, F. Piazza and M. Raghunath, Synergistic rate boosting of collagen fibrillogenesis in heterogeneous mixtures of crowding agents, *J. Phys. Chem. B*, 2015, **119**(12), 4350–4358.

32 J. D. Mott, C. L. Thomas, M. T. Rosenbach, K. Takahara, D. S. Greenspan and M. J. Banda, Post-translational proteolytic processing of procollagen C-terminal proteinase enhancer releases a metalloproteinase inhibitor, *J. Biol. Chem.*, 2000, **275**(2), 1384–1390.

33 F. Grinnell, Fibronectin and wound healing, *J. Cell Biochem.*, 1984, **26**(2), 107–116.

34 D. F. Mosher, Assembly of fibronectin into extracellular matrix, *Curr. Opin. Struct. Biol.*, 1993, **3**(2), 214–222.

35 V. Vogel, Mechanotransduction involving multimodular proteins: converting force into biochemical signals, *Annu. Rev. Biophys. Biomol. Struct.*, 2006, **35**, 459–488.

36 S. Fernandez-Sauze, D. Grall, B. Cseh and E. Van Obberghen-Schilling, Regulation of fibronectin matrix assembly and capillary morphogenesis in endothelial cells by Rho family GTPases, *Exp. Cell Res.*, 2009, **315**(12), 2092–2104.

37 P. Singh, C. Carraher and J. E. Schwarzbauer, Assembly of Fibronectin Extracellular Matrix, *Annu. Rev. Cell Dev. Biol.*, 2010, **26**(1), 397–419.

38 G. Baneyx and V. Vogel, Self-assembly of fibronectin into fibrillar networks underneath dipalmitoyl phosphatidylcholine monolayers: role of lipid matrix and tensile forces, *Proc. Natl. Acad. Sci. U. S. A.*, 1999, **96**(22), 12518–12523.

39 R. Pankov, E. Cukierman, B. Z. Katz, K. Matsumoto, D. C. Lin, S. Lin, *et al.*, Integrin dynamics and matrix assembly: tensin-dependent translocation of alpha(5)beta(1) integrins promotes early fibronectin fibrillogenesis, *J. Cell Biol.*, 2000, **148**(5), 1075–1090.

40 G. Baneyx, L. Baugh and V. Vogel, Fibronectin extension and unfolding within cell matrix fibrils controlled by cytoskeletal tension, *Proc. Natl. Acad. Sci. U. S. A.*, 2002, **99**(8), 5139–5143.

41 R. O. Hynes, The Extracellular Matrix: Not Just Pretty Fibrils, *Science*, 2009, **326**(5957), 1216–1219.

42 V. Vogel, Unraveling the Mechanobiology of Extracellular Matrix, *Annu. Rev. Physiol.*, 2018, **80**(1), 353–387.

43 J. A. McDonald, D. G. Kelley and T. J. Broekelmann, Role of fibronectin in collagen deposition: Fab' to the gelatin-binding domain of fibronectin inhibits both fibronectin and collagen organization in fibroblast extracellular matrix, *J. Cell Biol.*, 1982, **92**(2), 485–492.

44 J. Sottile and D. C. Hocking, Fibronectin Polymerization Regulates the Composition and Stability of Extracellular Matrix Fibrils and Cell-Matrix Adhesions, *Mol. Biol. Cell*, 2002, **13**(10), 3546–3559.

45 J. Sottile, F. Shi, I. Rublyevska, H.-Y. Chiang, J. Lust, J. Chandler, *et al.*, Fibronectin-dependent collagen I deposition modulates the cell response to fibronectin, *Am. J. Physiol.*, 2007, **293**(6), C1934–C1946.

 

46 K. E. Kadler, A. Hill and E. G. Canty-Laird, Collagen fibrillogenesis: fibronectin, integrins, and minor collagens as organizers and nucleators, *Curr. Opin. Cell Biol.*, 2008, **20**(5), 495–501.

47 K. E. Kubow, R. Vukmirovic, L. Zhe, E. Klotzsch, M. L. Smith, D. Gourdon, *et al.*, Mechanical forces regulate the interactions of fibronectin and collagen I in extracellular matrix, *Nat. Commun.*, 2015, **6**, 8026.

48 G. Huang, Y. Zhang, B. Kim, G. Ge, D. S. Annis, D. F. Mosher, *et al.*, Fibronectin Binds and Enhances the Activity of Bone Morphogenetic Protein 1, *J. Biol. Chem.*, 2009, **284**(38), 25879–25888.

49 J. T. Saunders and J. E. Schwarzbauer, Fibronectin matrix as a scaffold for procollagen proteinase binding and collagen processing, *Mol. Biol. Cell*, 2019, **30**(17), 2218–2226.

50 B. Fogelgren, N. Polgár, K. M. Szauter, Z. Újfaludi, R. Laczkó, K. S. K. Fong, *et al.*, Cellular Fibronectin Binds to Lysyl Oxidase with High Affinity and Is Critical for Its Proteolytic Activation, *J. Biol. Chem.*, 2005, **280**(26), 24690–24697.

51 K. E. Kubow, E. Klotzsch, M. L. Smith, D. Gourdon, W. C. Little and V. Vogel, Crosslinking of cell-derived 3D scaffolds up-regulates the stretching and unfolding of new extracellular matrix assembled by reseeded cells, *Integr. Biol.*, 2009, **1**(11–12), 635–648.

52 G. Baneyx, L. Baugh and V. Vogel, Coexisting conformations of fibronectin in cell culture imaged using fluorescence resonance energy transfer, *Proc. Natl. Acad. Sci. U. S. A.*, 2001, **98**(25), 14464–14468.

53 L. Baugh and V. Vogel, Structural changes of fibronectin adsorbed to model surfaces probed by fluorescence resonance energy transfer, *J. Biomed. Mater. Res., Part A*, 2004, **69**(3), 525–534.

54 M. L. Smith, D. Gourdon, W. C. Little, K. E. Kubow, R. A. Eguiluz, S. Luna-Morris, *et al.*, Force-induced unfolding of fibronectin in the extracellular matrix of living cells, *PLoS Biol.*, 2007, **5**(10), e268.

55 M. Antia, G. Baneyx, K. E. Kubow and V. Vogel, Fibronectin in aging extracellular matrix fibrils is progressively unfolded by cells and elicits an enhanced rigidity response, *Faraday Discuss.*, 2008, **139**, 229.

56 W. C. Little, M. L. Smith, U. Ebneter and V. Vogel, Assay to mechanically tune and optically probe fibrillar fibronectin conformations from fully relaxed to breakage, *Matrix Biol.*, 2008, **27**(5), 451–461.

57 E. Klotzsch, M. L. Smith, K. E. Kubow, S. Muntwyler, W. C. Little, F. Beyeler, *et al.*, Fibronectin forms the most extensible biological fibers displaying switchable force-exposed cryptic binding sites, *Proc. Natl. Acad. Sci. U. S. A.*, 2009, **106**(43), 18267–18272.

58 W. R. Legant, C. S. Chen and V. Vogel, Force-induced fibronectin assembly and matrix remodeling in a 3D microtissue model of tissue morphogenesis, *Integr. Biol.*, 2012, **4**(10), 1164–1174.

59 B. Li, C. Moshfegh, Z. Lin, J. Albuschies and V. Vogel, Mesenchymal Stem Cells Exploit Extracellular Matrix as Mechanotransducer, *Sci. Rep.*, 2013, **3**, 2425.

60 B. Li, Z. Lin, M. Mitsi, Y. Zhang and V. Vogel, Heparin-induced conformational changes of fibronectin within the extracellular matrix promote hMSC osteogenic differentiation, *Biomater. Sci.*, 2015, **3**(1), 73–84.

61 P. Kollmannsberger, C. M. Bidan, J. W. C. Dunlop, P. Fratzl and V. Vogel, Tensile forces drive a reversible fibroblast-to-myofibroblast transition during tissue growth in engineered clefts, *Sci. Adv.*, 2018, **4**(1), eaao4881.

62 D. Ortiz Franyuti, M. Mitsi and V. Vogel, Mechanical Stretching of Fibronectin Fibers Upregulates Binding of Interleukin-7, *Nano Lett.*, 2018, **18**(1), 15–25.

63 Z. Avnur and B. Geiger, The removal of extracellular fibronectin from areas of cell-substrate contact, *Cell*, 1981, **25**(1), 121–132.

64 D. M. Peters, L. M. Portz, J. Fullenwider and D. F. Mosher, Co-assembly of plasma and cellular fibronectins into fibrils in human fibroblast cultures, *J. Cell Biol.*, 1990, **111**(1), 249–256.

65 S. K. Mitra, D. A. Hanson and D. D. Schlaepfer, Focal adhesion kinase: in command and control of cell motility, *Nat. Rev. Mol. Cell Biol.*, 2005, **6**(1), 56–68.

66 J. S. Kim and A. Yethiraj, Crowding effects on association reactions at membranes, *Biophys. J.*, 2010, **98**(6), 951–958.

67 R. Chapanian, D. H. Kwan, I. Constantinescu, F. A. Shaikh, N. A. A. Rossi, S. G. Withers, *et al.*, Enhancement of biological reactions on cell surfaces via macromolecular crowding, *Nat. Commun.*, 2014, **5**, 4683.

68 M. Chabria, S. Hertig, M. L. Smith and V. Vogel, Stretching fibronectin fibres disrupts binding of bacterial adhesins by physically destroying an epitope, *Nat. Commun.*, 2010, **1**(9), 135.

69 S. Hertig, M. Chabria and V. Vogel, Engineering Mechanosensitive Multivalent Receptor–Ligand Interactions: Why the Nanolinker Regions of Bacterial Adhesins Matter, *Nano Lett.*, 2012, **12**(10), 5162–5168.

70 S. M. Früh, I. Schoen, J. Ries and V. Vogel, Molecular architecture of native fibronectin fibrils, *Nat. Commun.*, 2015, **6**(1), 7275.

71 E. G. Hayman, Distribution of fetal bovine serum fibronectin and endogenous rat cell fibronectin in extracellular matrix, *J. Cell Biol.*, 1979, **83**(1), 255–259.

72 A. Satyam, P. Kumar, D. Cigognini, A. Pandit and D. I. Zeugolis, Low, but not too low, oxygen tension and macromolecular crowding accelerate extracellular matrix deposition in human dermal fibroblast culture, *Acta Biomater.*, 2016, **44**, 221–231.

73 M. Patrikoski, M. H. C. Lee, L. Mäkinen, X. M. Ang, B. Mannerström, M. Raghunath, *et al.*, Effects of Macromolecular Crowding on Human Adipose Stem Cell Culture in Fetal Bovine Serum, Human Serum, and Defined Xeno-Free/Serum-Free Conditions, *Stem Cells Int.*, 2017, **2017**, 6909163.

74 T. P. Ugarova, C. Zamarron, Y. Veklich, R. D. Bowditch, M. H. Ginsberg, J. W. Weisel, *et al.*, Conformational Transitions in the Cell Binding Domain of Fibronectin, *Biochemistry*, 1995, **34**(13), 4457–4466.